Chapter 1. Molecular Biology of the Circadian Rhythm in *Drosophila*

Circadian rhythms in *Drosophila* and *Neurospora* have been studied intensively at the molecular level. The *per* gene of *Drosophila* was discovered in 1971 by Konopka and Benzer (Konopka and Benzer, 1971). *per* mRNA and PER protein levels oscillate with a circadian rhythm (Hardin et al., 1990; Zeng et al., 1994). Mutations of the *per* gene cause abnormal circadian rhythms of *Drosophila*'s locomotor activity and its eclosion timing (Loros et al., 1989). The *per* null mutation (per^0) causes arrhythmic behavior, and *per* missense mutations can either shorten (per^S) or lengthen (per^L) the period of circadian rhythms (Huang et al., 1995). The per^S mutant has a period of 19 hours, and the per^L mutant has a period of 27 hours at 18C. A remarkable observation of the per^L mutant is that its period is sensitive to temperature changes (Huang et al., 1995). The per^L mutant has a 25 hour rhythm at 15C and a 33 hour rhythm at 30C. Its period increases markedly with increasing temperature.

The protein product of *per* seems to regulate its own expression. Based on studies of PER protein and *per* mRNA levels, scientists were able to show that PER is a nuclear protein (Curtin et al., 1995), and that PER acts as a negative regulator of its own transcription, forming an autoregulatory negative feedback loop (Hardin et al. 1990). PER protein level parallels *per* mRNA level with several hours delay (about 4-6 hrs) indicating that there are post-transcriptional control mechanisms that come into play (Hardin et al., 1990; Zeng et al., 1995). As PER accumulates, it becomes progressively phosphorylated (Edery et al., 1994), and it is translocated from the cytoplasm to the nucleus, which suggests a possible negative feedback loop (Curtin et al., 1995). Moreover, overexpression of PER suppresses *per* mRNA cycling in photoreceptor cells, providing more evidence of PER negatively regulating its own transcription (Zeng et al., 1994).

In 1994, a new *Drosophila* gene, *timeless* (*tim*), was identified (Sehgal et al., 1994). Similar to the *per* null mutant (per^0), the *tim* null mutation (tim^0) abolishes circadian rhythms of *Drosophila*'s locomotor and eclosion activities. The tim^0 mutation eliminates the circadian oscillation of *per* mRNA, indicating an interaction between *per* and *tim*.

Co-immunoprecipitation experiments have shown that TIM protein can physically interact with PER (Gekakis et al., 1995; Myers et al., 1995; Sehgal et al., 1995; Sehgal et

al., 1994; Vosshall et al., 1994; Zeng et al., 1996), and this interaction seems to be necessary for translocation of both proteins from the cytoplasm to the nucleus. *tim* and *per* mRNA levels are indistinguishable from each other in wild type flies (Sehgal et al., 1995). More interestingly, *tim* mRNA levels are also identical with *per* mRNA in per^S mutants, and *tim* mRNA oscillation is abolished in per^0 (Sehgal et al., 1995). In per^L mutant flies, the interaction between PER and TIM is disrupted with increasing temperature (Gekakis et al., 1995). This suggests that PER-TIM hetero-interaction is a part of the temperature compensation mechanism, and its dirsuption may cause a delay of the rhythm.

TIM protein seems to be responsible for the phase shift caused by light. In *Drosophila*, degradation of TIM protein is induced by light pulses (Hunter-Ensor et al., 1996; Lee et al., 1996; Myers et al., 1996; Zeng et al., 1996). TIM degradation disrupts PER and TIM interaction and either delays or advances the rhythm depending on when the light pulse is applied. This evidence suggests that light resets the circadian clock by destroying TIM. This makes sense because as light destroys TIM, PER will not be able to get into the nucleus on time, and its negative feedback loop will be either delayed or advanced.

The transcriptional activation of *per* and *tim* seems to be activated by positive elements of the clock called JRK and CYC (Allada et al., 1998; Darlington et al., 1998; Rutila et al., 1998). They are transcription factors which drive the transcription of clock genes *per* and *tim*. PER and TIM proteins then feed back into the nucleus and bind to JRK and CYC, and inhibit their own activation. Mutations in both genes (*jrk* and *cyc*) abolish the expression of *per* and *tim*.

Last summer, another novel circadian rhythm gene, *doubletime* (*dbt*), was isolated (Kloss et al., 1998; Price et al., 1998). It codes for DBT protein, which is a casein-like kinase. DBT protein phosphorylates monomeric PER protein and decreases its stability. However, as soon as monomeric PER forms a heterodimer with TIM, it becomes much more stable. Three mutant phenotypes of the *dbt* gene have been identified. dbt^P is null mutation and codes for nonfunctional DBT protein, which leads to an accumulation of the hypophosphorylated form of monomeric PER. This stabilization of PER abolishes the rhythm by constantly inhibiting its own transcription. dbt^S has a shorter period of 18

hours (homozygote) with increased kinase activity, and dbt^{L} has a longer period of 26.8 hours (homozygote) with decreased kinase activity.

The consensus opinion is that the circadian rhythm in *Drosophila* is based on a negative feedback mechanism governed by PER and TIM. Here we propose that there is a positive feedback loop, based on stabilization of PER upon dimerization with TIM, which works in concert with the negative feedback loop to generate the circadian rhythm.

There is no doubt that these components (PER, TIM, JRK, CYC, and DBT) play major roles in the circadian rhythm mechanism. However, there are probably more components to be identified. Although the actual clock mechanism may be much more complex, involving other clock genes which are not yet identified, enough is known to build preliminary mathematical models which may explain many physiological and molecular properties of circadian rhythms and provide a framework for more complex, realistic mechanisms.

Chapter 2. A Model of the Circadian Rhythm Based on Heterodimerization of PER and TIM

The experimental results described in chapter 1 led some theoreticians to propose a mechanism of circadian rhythms based on the negative feedback loop of PER inhibiting its own transcription (Goldbeter, 1995; Ruoff and Rensing, 1996). In 1995, Albert Goldbeter proposed a "minimal" model for circadian oscillations (Fig. 2.1). This model is described by the following equations:

(1a) $$\frac{dM}{dt} = v_s \frac{K_I^n}{K_I^n + P_N^n} - v_m \frac{M}{K_m + M}$$

(1b) $$\frac{dP_0}{dt} = k_s M - V_1 \frac{P_0}{K_1 + P_0} + V_2 \frac{P_1}{K_2 + P_1}$$

(1c) $$\frac{dP_1}{dt} = V_1 \frac{P_0}{K_1 + P_0} - V_2 \frac{P_1}{K_2 + P_1} - V_3 \frac{P_1}{K_3 + P_1} + V_4 \frac{P_2}{K_4 + P_2}$$

(1d) $$\frac{dP_2}{dt} = V_3 \frac{P_1}{K_3 + P_1} - V_4 \frac{P_2}{K_4 + P_2} - k_{in} P_2 + k_{out} P_N - v_d \frac{P_2}{K_d + P_2}$$

(1e) $$\frac{dP_N}{dt} = k_{in} P_2 - k_{out} P_N$$

For simplicity, Goldbeter assumed that the rate of PER synthesis (dP_0/dt) is proportional to the supply of *per* mRNA (M), and that there are only two phosphorylation steps before PER can be translocated into the nucleus. He assumed that the doubly phosphorylated form of PER (P_2) is unstable, but the unphosphorylated (P_0), monophosphorylated (P_1), and nuclear (P_N) forms are stable. *per* mRNA is also enzymatically degraded. With these assumptions and appropriate parameter values, he showed that the mechanism generates sustained oscillations in PER protein and *per* mRNA, corresponding to a limit cycle surrounding an unstable steady state (Fig. 2.2).

Goldbeter's model accounted for many characteristic features of circadian oscillations, such as its 24 hour free-running period, but did not address the issue of temperature compensation nor the phase shift caused by light. However, in that same year, Gekakis et al. suggested a possible temperature compensation mechanism through heterotypic interaction between PER and TIM based on the disruption of PER and TIM dimerization in per^L in high temperatures (Gekakis et al., 1995). TIM seems to control the nuclear

entry of PER, because in the absence of TIM, PER does not undergo nuclear translocation (Gekakis et al., 1995).

In 1997, prompted by Gekakis' results and suggestions, we proposed that, as temperature increases, the rate of nuclear entry (k_{in}) decreases and the period of oscillation increases, because more time is required to accumulate enough PER in the nucleus to inhibit the transcription of *per*. In order to compensate for the decreased rate of PER entry to the nucleus at higher temperature, we assume that the rate of hetero-dimerization (k_{assoc}) of PER and TIM increases with temperature and provides a faster movement of the protein for nuclear entry of PER-TIM heterodimer. Incorporating this new information, we obtained a schematic diagram shown in Fig. 2.3, and corresponding equations in Fig. 2.4.

In this model, we assume that only doubly phosphorylated PER-TIM dimers enter the nucleus, and that PER-TIM dimers in the nucleus do not move back into the cytoplasm. Once these dimers are in the nucleus, they inhibit transcription of the *per* and *tim* genes.

Mutants (per^L) with reduced dimerization show longer periods of oscillation with increasing temperature. This could be the result of changes in many different combinations of rate constants in the model, most notably by k_{assoc} and k_{in}. To represent this effect, we assume that k_{in} decreases with temperature (Fig. 2.5), causing an increase of circadian period (Fig. 2.6, solid curve) in mutant flies (k_{assoc} small). For wild-type flies, we suppose that k_{assoc} which is the dimerization rate constant, increases with temperature (Fig. 2.5). Therefore by adjusting the temperature dependencies of k_{assoc} and k_{in}, we can maintain 24-hour periodicity (Fig. 2.6, dashed curve). In this model, increased dimerization reaction rate constant speeds up the oscillation in order to compensate for the delay caused by the decrease of the rate of nuclear entry.

This model was primitive in a sense, because there were too many assumptions: the rate of nuclear entry (k_{in}) decreases with increasing temperature, only the rate of dimerization (k_{assoc}) increases with increasing temperature, and the protein is not able to move out from the nucleus. Also, this model did not account for phase shift caused by light upon TIM degradation. The next model, in chapter 3, will deal with a more realistic picture of the circadian rhythm mechanism that suggests a simpler model.

Chapter 3. A Simple Model of Circadian Rhythms Based on Dimerization and Proteolysis of PER and TIM

Identification of the novel circadian gene, *dbt*, and the function of DBT protein, gave more insight to the mechanism of circadian rhythms in Drosophila (Kloss et al., 1998; Price et al., 1998). Different proteolysis rates between monomeric PER and PER-TIM heterodimer upon phosphorylation by kinase, DBT, suggested a mechanism in which PER protects itself from degradation. It was shown that monomeric PER is more susceptible to proteolysis upon phosphorylation by DBT (Kloss et al., 1998; Price et al., 1998). In contrast, PER-TIM heterodimer is rather stable, and translocates into the nucleus. In other words, as PER increases, there is more of a chance to form a heterodimer with TIM, and escape from proteolysis activated by DBT. This implies a positive feedback mechanism because the total concentration of PER increases nonlinearly, as PER inhibits its own degradation.

The mechanism in Fig. 3.1 summarizes the properties of PER, TIM, and DBT, and their negative and positive feedback mechanisms. This can be converted into six differential equations explaining the rate of changes of *per* and *tim* mRNA, PER and TIM monomeric protein, PER-TIM heterodimer in the cytoplasm and in the nucleus. This set of equations can be put into the computer, and simulated to observe how it behaves for different parameter values. The difficulty lies in trying to follow the positive feedback mechanism in such a complicated system. So we decided to reduce this model to a simpler picture by lumping together *per* and *tim* mRNA, and PER and TIM proteins (knowing that they follow similar time courses). We also assumed that dimer formation is fast. This simplified mechanism (Fig. 3.2) is converted into the following three differential equations.

$$\frac{dM}{dt} = \frac{v_m}{1 + \left(\frac{P_t}{P_{crit}}\right)^2} - k_m M \qquad [1]$$

$$\frac{\mathrm{d}P_1}{\mathrm{d}t} = v_p M - \frac{k_{p1} P_1}{J_p + P_1 + 2P_2} - k_{p3} P_1 - 2k_a P_1^{\,2} + 2k_d P_2 \qquad [2]$$

$$\frac{dP_2}{dt} = k_a P_1^2 - k_d P_2 - \frac{k_{p2} P_2}{J_p + P_1 + 2P_2} - k_{p3} P_2 \qquad [3]$$

The rates of change of mRNA, protein, and dimerized protein are denoted as dM/dt, dP_1/dt, and dP_2/dt, respectively. The message is transcribed with a maximal rate of v_m and inhibited by PER/TIM heterodimers, and proportionally degraded (k_m) depending on its own concentration. We assume a Hill coefficient of 2, which represents some cooperativity for the inhibition of negative feedback loop. This assumption enables the model to describe more properties of mutants. Monomer proteins are synthesized proportionally with the concentration of mRNA, and degraded or associated with other monomer protein to form dimer. Dimers are formed from the association of monomers, and they can also be degraded or lost by dissociation. Both monomers and dimers are also able to bind to DBT, and be degraded upon phosphorylation. However, based on evidence, we assume that P_1 is more susceptible to phosphorylation and degrades rapidly, and P_2 is less susceptible to phosphorylation ($k_{p1} >> k_{p2}$). Notice also that P_2 is a competitive inhibitor of P_1 phosphorylation.

This set of three differential equations can be reduced to two differential equations by expressing P_1 and P_2 as functions of total protein ($P_t = P_1 + 2P_2$). If the dimerization reactions are fast enough, P_1 and P_2 will be always in equilibrium with each other. If we let $K_{eq} = \frac{P_2}{P_1^2}$ and $q = \frac{P_1}{P_t}$, we can get $P_2 = \frac{1}{2}(1-q)P_t$ and $q = \frac{2}{1+\sqrt{1+8K_{eq}P_t}}$. Based on these facts, we can reduce the original set of three differential equations into the following two differential equations:

$$\frac{dM}{dt} = \frac{v_m}{1 + \left(\frac{P_t(1-q)}{2P_{crit}}\right)^2} - k_m M \qquad [4]$$

$$\frac{dP_t}{dt} = v_p M - \frac{k'_{p1} P_t q + k_{p2} P_t}{J_p + P_t} - k_{p3} P_t \qquad [5]$$

where $k_{p1}' = k_{p1} - k_{p2}$, and k_{p2} is significantly smaller then k_{p1}.

If we choose the right parameter values (Table 3.1), it is possible to generate a 24 hour free-running cycle of mRNA and protein (Fig. 3.3). The protein peak is delayed about 7 hours after peak mRNA level. This result is somewhat different from the experimental observation that PER protein is delayed about 4-6 hours after mRNA.

Table 3.1. Parameter values for circadian rhythm of wild-type fruit flies

Name	Value	Units *	Description
v_m	1	$C_m\ h^{-1}$	Maximum rate of synthesis of mRNA
k_m	0.1	h^{-1}	First-order rate const for mRNA degrad'n
v_p	0.5	$C_p\ C_m^{-1}\ h^{-1}$	Rate constant for translation of mRNA
k_{p1}'	10	$C_p\ h^{-1}$	V_{max} for monomer phosphorylation
k_{p2}	0.03	$C_p\ h^{-1}$	V_{max} for dimer phosphorylation
k_{p3}	0.1	h^{-1}	First-order rate const for proteolysis
K_{eq}	200	C_p^{-1}	Equilibrium constant for dimerization
P_{crit}	0.1	C_p	Dimer concen at half-maximal transcr'n rate
J_p	0.05	C_p	Michaelis constant for protein kinase (DBT)

* C_m and C_p represent characteristic concentrations for mRNA and protein, respectively.

Our model can also account for phase shift properties of circadian rhythms in response to light pulses in constant darkness. From the evidence of TIM protein degradation upon the light pulse causing disruption of PER-TIM heterodimerization (Hunter-Ensor et al., 1996; Lee et al., 1996; Myers et al., 1996; Zeng et al., 1996), we assume that a light pulse reduces the equilibrium binding rate constant K_{eq}. With this assumption, we were able to generate typical phase response curves (Fig. 3.4) indicating phase delays and advances depending on when the light pulse was applied. This is done by simulating the model with either 10 minutes or 30 minutes of reduced K_{eq} in different time intervals, and putting back to high K_{eq}. Figure 3.4 shows qualitatively similar results as in experiments (Myers et al., 1996; Pittendrigh, 1967), but they are quantitatively quite different, because

our simulation fails to generate a long phase where the clock is not influenced by light pulse, as previously noted in experiments.

In addition, our model can simulate the light entrainment property of circadian rhythm, which adapts to the external light-dark period (Fig. 3.5). This simulation indicates that in order to entrain the rhythm of an organism, the amplitude of external signal must be larger as its period deviates further from the endogenous period of the circadian rhythm.

The benefit of having just a pair of differential equations is that the dynamical system can be portrayed in the phase plane (Edelstein-Keshet, 1988). A point in the positive quadrant of the phase plane (Fig. 3.6) represents a biochemical state of the control system (i.e. instantaneous concentrations of mRNA and total protein). On the phase plane we draw two "nullclines." The M-nullcline is the locus of states where mRNA synthesis is exactly balanced by degradation. In other words, on its nullcline, mRNA does not experience any net change caused by its own synthesis or degradation, and the only change comes from the protein component. The P-nullcline is described similarly. The M and P nullclines are given by the following equations:

$$M = \frac{v_m}{k_m}\left[1 + \left(\frac{P_t(1-q)}{2P_{crit}}\right)^2\right]^{-1} \qquad \text{[M-nullcline]}$$

$$M = \frac{k_{p1}P_t q + k_{p2}P_t}{v_p(J_p + P_t)} + \frac{k_{p3}P_t}{v_p} \qquad \text{[P-nullcline]}$$

Because negative feedback inhibition by dimers is cooperative, the M-nullcline decreases dramatically at high protein concentration, as indicated by its sigmoidal shape. The P-nullcline is N-shaped because of the positive feedback loop caused by formation of dimers, which inhibits the degradation of monomers.

With the parameter values in Table 3.1,the M- and P- nullclines intersect at an unstable steady state, creating a stable limit cycle with period close to 24 hours. If we change the parameter values in order to simulate mutants, the system may change the period of oscillation or abolish the rhythm and converge to stable steady state (Fig. 3.7).

In Fig. 3.8, we indicate how our model behaves upon variations of equilibrium binding constant (K_{eq}), and monomeric protein degradation rate (k_{p1}). Stable limit cycles exist

within the U-shaped region where the system has an unstable steady state. It is also shown that there exist different periods of oscillations depending on K_{eq} and k_{p1}. We assume that the wild type control system has high K_{eq} where period is quite insensitive to the changes in both K_{eq} and k_{p1}, while the per^L mutant lies in the region of low K_{eq} where period is sensitive to changes in K_{eq} and k_{p1}. This is in accordance with the experimental results, because it is known that per^L is less efficient to form dimers, which leads to increased activity of degradation of monomeric proteins, and causes increased period.

Conclusion

Our model of circadian rhythms in *Drosophila* has evolved as new experimental facts have been published. At first, we accepted the idea of a biochemical oscillator based on negative feedback, and we tried to build a better model which could explain temperature compensation of circadian rhythms and mutant phenotypes of fruit fly. Knowing that there are more ways to make a biochemical clock, we later speculated if negative feedback is the only way to build a circadian oscillator. We proposed that there could be a major role for a positive feedback loop generated by PER-TIM heterodimer formation inhibiting PER degradation. From this perspective, we suspect that the mechanism of circadian rhythms in *Drosophila* is a concert of both negative and positive feedback mechanisms.

Our model is yet too simple, and cannot simulate the exact properties of the circadian rhythm in fruit flies, such as the precise shapes of phase response curves, and the time delay between mRNA and protein peaks. Because it describes the principal roles of protein synthesis, phosphorylation, dimerization, and proteolysis in the system, this simple model provides the basic foundation for building a more comprehensive model of circadian rhythms.

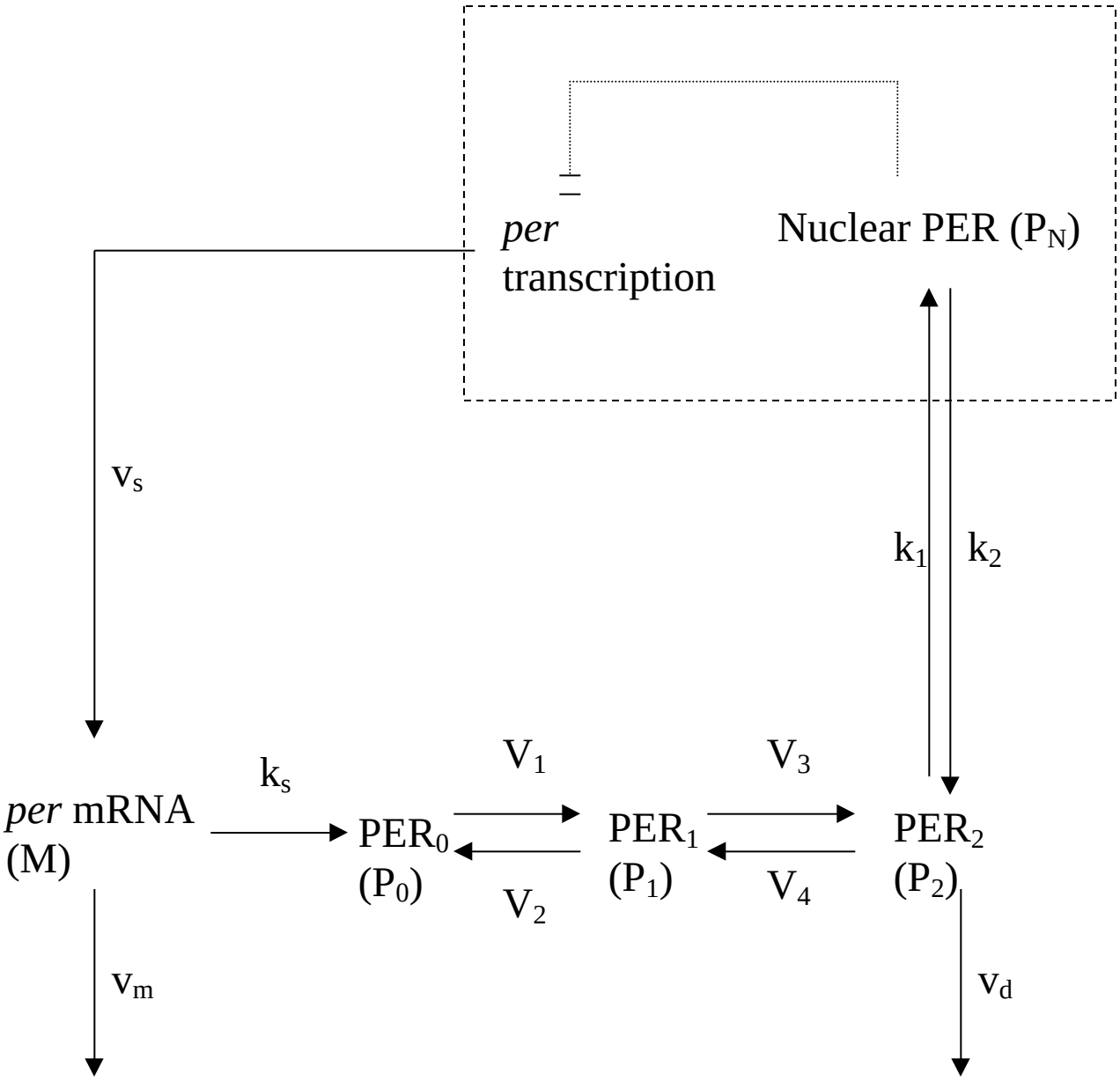

Fig. 2.1. A molecular mechanism of the circadian clock in *Drosophila* based on negative feedback (Goldbeter, 1995). The *per* mRNA (M) is transcribed in the nucleus, and translated to PER in the cytoplasm where it accumulates at a maximum rate v_s, and is degraded by an enzyme of maximum rate v_m and Michaelis constant k_m. PER protein is synthesized at a rate proportional to its mRNA concentration and subjected to phosphorylation. Both phosphorylation and dephosphorylation are carried out with maximum rate v_i and Michaelis constant K_i (i = 1, …4). The doubly phosphorylated PER

is degraded at a maximum rate of v_d and Michaelis constant k_d, and transported into the nucleus at a rate of k_1. The negative feedback loop is characterized by the Hill type equation (equation 1a) of PER inhibiting *per* transcription in which n denotes the degree of cooperativity and K_I the threshold constant for repression.

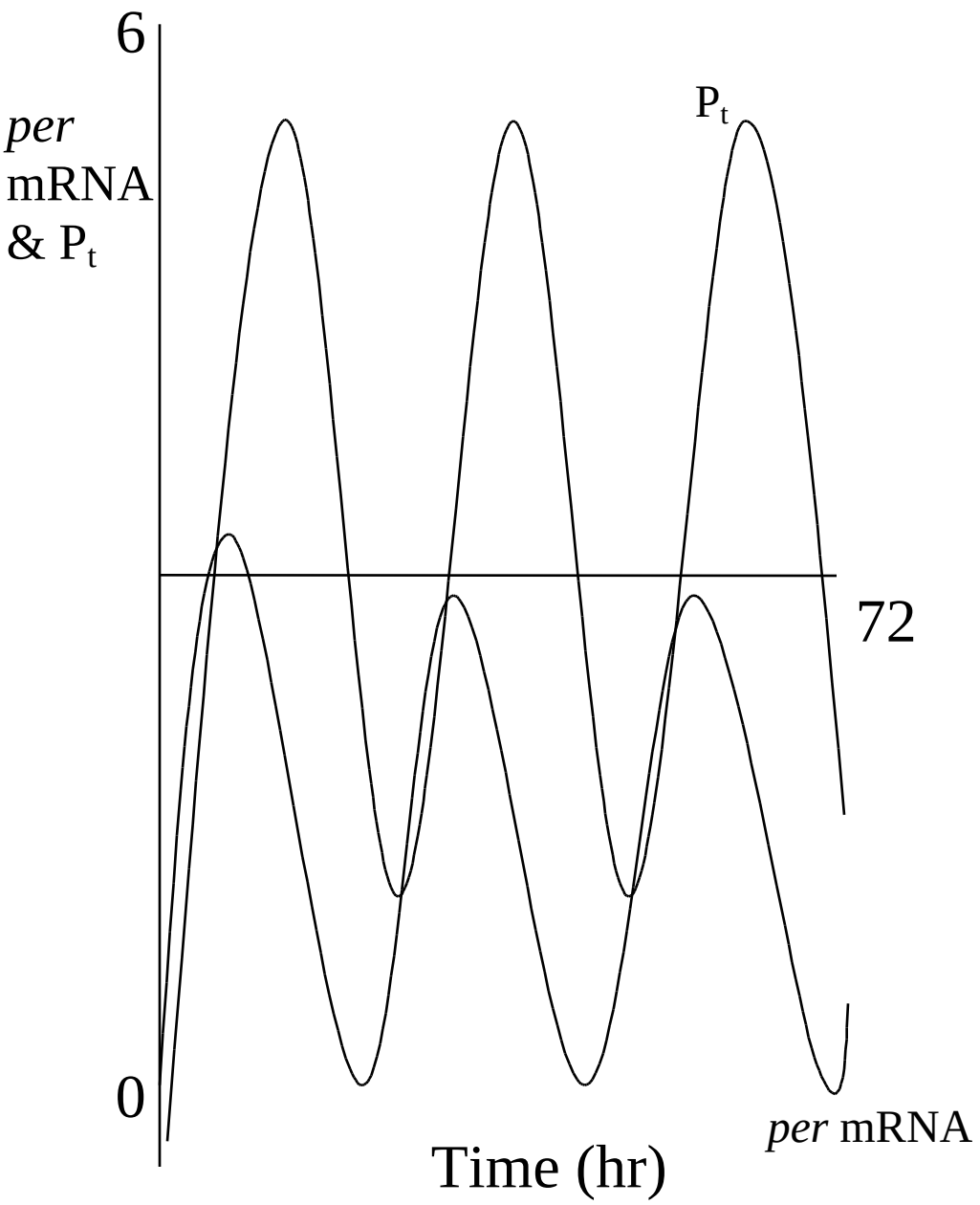

Fig. 2.2. Numerical solution of Goldbeter's model (Goldbeter, 1995). Parameter values: v_s = 0.76 μM h^{-1}, v_m = 0.65 μM h^{-1}, k_m = 0.5 μM, k_s = 0.38 h^{-1}, v_d = 0.95 μM h^{-1}, k_{in} = 1.9 h^{-1}, k_{out} = 1.3 h^{-1}, K_I = 1 μM, k_d = 0.2 μM, n = 4, $K_1 = K_2 = K_3 = K_4$ = 2 μM, V_1 = 3.2 μM h^{-1}, V_2 = 1.58 μM h^{-1}, V_3 = 5 μM h^{-1}, V_4 = 2.5 μM h^{-1}.

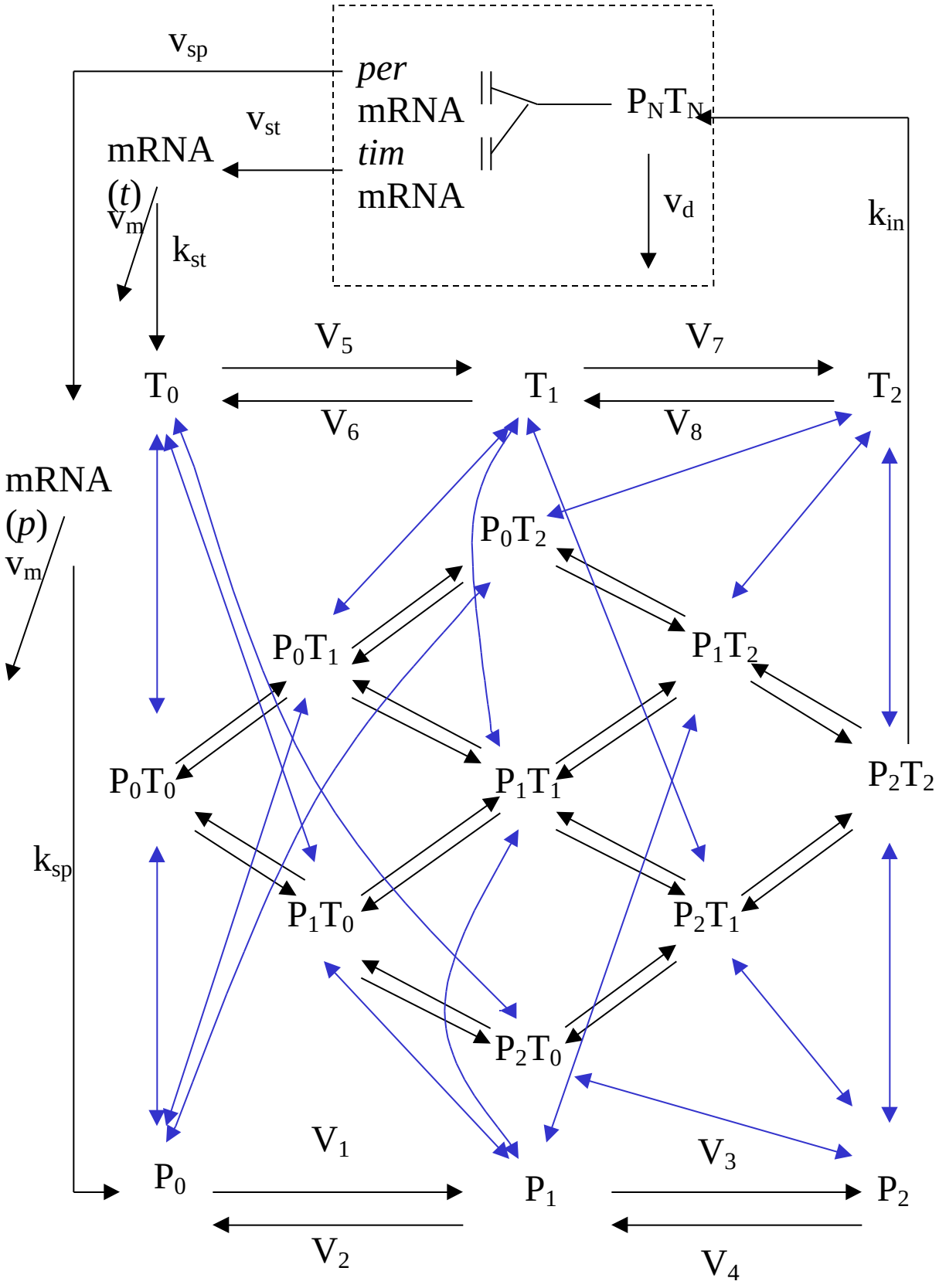

Fig. 2.3. A mechanism for circadian oscillations based on PER-TIM heterodimerization. The notation is identical to Fig. 2.1 with the addition of two parameters: k_{assoc} and k_{dissoc},

denoting the rate constants for dimer association and dissociation, respectively. Both monomer and dimer forms of PER and TIM in the cytoplasm are degraded by first order kinetics. The phosphorylation and dephosphorylation reactions follow Michaelis-Menten kinetics. The fully phosphorylated form of heterodimer is transported into the nucleus, and within the nucleus it inhibits its own transcription or is degraded by Michaelis-Menten kinetics. Blue arrows indicate the association and dissociations of the proteins.

Fig. 2.4. Differential equations implied by Fig. 2.3.

(2a) $$\frac{\mathrm{d}MP}{\mathrm{d}t} = v_{sp}\frac{1}{1+(P_N T_N)^n} - v_{mp}\frac{MP}{K_{mp}+MP}$$

(2b) $$\frac{\mathrm{d}MT}{\mathrm{d}t} = v_{st}\frac{1}{1+(P_N T_N)^n} - v_{mt}\frac{MT}{K_{mt}+MT}$$

(2c) $$\frac{\mathrm{d}P_0}{\mathrm{d}t} = k_{sp}MP - V_1\frac{P_0}{K_1+P_0} + V_2\frac{P_1}{K_2+P_1} - k_{cyt}P_0 - k_{assoc}P_0T_0 + k_{dissoc}(P_0T_0) - k_{assoc}P_0T_1 + k_{dissoc}(P_0T_1) - k_{assoc}P_0T_2 + k_{dissoc}(P_0T_2)$$

(2d) $$\frac{\mathrm{d}P_1}{\mathrm{d}t} = V_1\frac{P_0}{K_1+P_0} - V_2\frac{P_1}{K_2+P_1} - V_3\frac{P_1}{K_3+P_1} + V_4\frac{P_2}{K_4+P_2} - k_{cyt}P_1 - k_{assoc}P_1\ T_0 + k_{dissoc}\ (P_1T_0) - k_{assoc}P_1\ T_1 + k_{dissoc}\ (P_1T_1) + k_{assoc}P_1\ T_2 - k_{dissoc}\ (P_1T_2)$$

(2e) $$\frac{\mathrm{d}P_2}{\mathrm{d}t} = V_3\frac{P_1}{K_3+P_1} - V_4\frac{P_2}{K_4+P_2} - k_{cyt}P_2 - k_{assoc}P_2\ T_0 + k_{dissoc}\ (P_2T_0) - k_{assoc}P_2\ T_1 + k_{dissoc}\ (P_2T_1) - k_{assoc}P_2\ T_2 - k_{dissoc}\ (P_2T_2)$$

(2f) $$\frac{\mathrm{d}T_0}{\mathrm{d}t} = k_{st}MT - V_5\frac{T_0}{K_5+T_0} + V_6\frac{T_1}{K_6+T_1} - k_{cyt}T_0 - k_{assoc}P_0\ T_0 + k_{dissoc}\ (P_0T_0) - k_{assoc}P_1T_0 + k_{dissoc}(P_1T_0) - k_{assoc}P_2T_0 + k_{dissoc}(P_2T_0)$$

(2g) $$\frac{\mathrm{d}T_1}{\mathrm{d}t} = V_5\frac{T_0}{K_5+T_0} - V_6\frac{T_1}{K_6+T_1} - V_7\frac{T_1}{K_7+T_1} + V_8\frac{T_2}{K_8+T_2} - k_{cyt}T_1 - k_{assoc}P_0\ T_1 + k_{dissoc}\ (P_0T_1) - k_{assoc}P_1\ T_1 + k_{dissoc}\ (P_1T_1) + k_{assoc}P_2\ T_1 - k_{dissoc}\ (P_2T_1)$$

(2h) $$\frac{\mathrm{d}T_2}{\mathrm{d}t} = V_7\frac{T_1}{K_7+T_1} - V_8\frac{T_2}{K_8+T_2} - k_{cyt}T_2 - k_{assoc}P_0\ T_2 + k_{dissoc}\ (P_0T_2) - k_{assoc}P_1\ T_2 + k_{dissoc}\ (P_1T_2) - k_{assoc}P_2\ T_2 - k_{dissoc}\ (P_2T_2)$$

(2i) $$\frac{\mathrm{d}P_0T_0}{\mathrm{d}t} = k_{assoc}P_0\ T_0 - k_{dissoc}\ (P_0T_0) - V_9\frac{P_0T_0}{K_9+P_0T_0} + V_{10}\frac{P_0T_1}{K_{10}+P_0T_1} - V_{11}\frac{P_0T_0}{K_{11}+P_0T_0} + V_{12}\frac{P_1T_0}{K_{12}+P_1T_0} - k_{cyt}P_0T_0$$

$$\frac{dP_0T_1}{dt} = k_{assoc}P_0\ \ T_1 - k_{dissoc}\ \ (P_0T_1) + V_9\frac{P_0T_0}{K_9 + P_0T_0} - V_{10}\frac{P_0T_1}{K_{10} + P_0T_1}$$

(2j)

$$- V_{13}\frac{P_0T_1}{K_{13} + P_0T_1} + V_{14}\frac{P_0T_2}{K_{14} + P_0T_2} - V_{15}\frac{P_0T_1}{K_{15} + P_0T_1} - V_{16}\frac{P_1T_1}{K_{16} + P_1T_1} - k_{cyt}P_0T_1$$

$$\frac{dP_1T_0}{dt} = k_{assoc}P_1\ \ T_0 - k_{dissoc}\ \ (P_1T_0) + V_{11}\frac{P_0T_0}{K_{11} + P_0T_0} - V_{12}\frac{P_1T_0}{K_{12} + P_1T_0}$$

(2k)

$$- V_{17}\frac{P_1T_0}{K_{17} + P_1T_0} + V_{18}\frac{P_1T_1}{K_{18} + P_1T_1} - V_{19}\frac{P_1T_0}{K_{19} + P_1T_0} - V_{20}\frac{P_2T_0}{K_{20} + P_2T_0} - k_{cyt}P_1T_0$$

$$\frac{dP_0T_2}{dt} = k_{assoc}P_0\ \ T_2 - k_{dissoc}\ \ (P_0T_2) + V_{13}\frac{P_0T_1}{K_{13} + P_0T_1} - V_{14}\frac{P_0T_2}{K_{14} + P_0T_2}$$

(2l)

$$- V_{21}\frac{P_0T_2}{K_{21} + P_0T_2} + V_{22}\frac{P_1T_2}{K_{22} + P_1T_2} - k_{cyt}P_0T_2$$

$$\frac{dP_1T_1}{dt} = k_{assoc}P_1\ \ T_1 - k_{dissoc}\ \ (P_1T_1) + V_{15}\frac{P_0T_1}{K_{15} + P_0T_1} - V_{16}\frac{P_1T_1}{K_{16} + P_1T_1}$$

(2m)

$$+ V_{17}\frac{P_1T_0}{K_{17} + P_1T_0} - V_{18}\frac{P_1T_1}{K_{18} + P_1T_1} - V_{23}\frac{P_1T_1}{K_{23} + P_1T_1} + V_{24}\frac{P_1T_2}{K_{24} + P_1T_2}$$

$$- V_{25}\frac{P_1T_1}{K_{25} + P_1T_1} + V_{26}\frac{P_2T_1}{K_{26} + P_2T_1} - k_{cyt}P_1T_1$$

$$\frac{dP_2T_0}{dt} = k_{assoc}P_2\ \ T_0 - k_{dissoc}\ \ (P_2T_0) + V_{19}\frac{P_1T_0}{K_{19} + P_1T_0} - V_{20}\frac{P_2T_0}{K_{20} + P_2T_0}$$

(2n)

$$- V_{27}\frac{P_2T_0}{K_{27} + P_2T_0} + V_{28}\frac{P_2T_1}{K_{28} + P_2T_1} - k_{cyt}P_2T_0$$

$$\frac{dP_1T_2}{dt} = k_{assoc}P_1\ \ T_2 - k_{dissoc}\ \ (P_1T_2) + V_{21}\frac{P_0T_2}{K_{21} + P_0T_2} - V_{22}\frac{P_1T_2}{K_{22} + P_1T_2}$$

(2o)

$$+ V_{23}\frac{P_1T_1}{K_{23} + P_1T_1} - V_{24}\frac{P_1T_2}{K_{24} + P_1T_2} - V_{29}\frac{P_1T_2}{K_{29} + P_1T_2} + V_{30}\frac{P_2T_2}{K_{30} + P_2T_2}$$

$$- k_{cyt}P_1T_2$$

$$\frac{dP_2T_1}{dt} = k_{assoc}P_2\ \ T_1 - k_{dissoc}\ \ (P_2T_1) + V_{25}\frac{P_1T_1}{K_{25} + P_1T_1} - V_{26}\frac{P_2T_1}{K_{26} + P_2T_1}$$

(2p)

$$+ V_{27}\frac{P_2T_0}{K_{27} + P_2T_0} - V_{28}\frac{P_2T_1}{K_{28} + P_2T_1} - V_{31}\frac{P_2T_1}{K_{31} + P_2T_1} + V_{32}\frac{P_2T_2}{K_{32} + P_2T_2}$$

$$- k_{cyt}P_2T_1$$

(2q)
$$\frac{dP_2T_2}{dt} = k_{assoc}P_2 \quad T_2 - k_{dissoc} \quad (P_2T_2) + V_{29}\frac{P_1T_2}{K_{29} + P_1T_2} - V_{30}\frac{P_2T_2}{K_{30} + P_2T_2}$$
$$+ V_{31}\frac{P_2T_1}{K_{31} + P_2T_1} - V_{32}\frac{P_2T_2}{K_{32} + P_2T_2} - k_{in} \quad (P_2T_2) - k_{cyt}P_2T_2$$

(2r)
$$\frac{dP_NT_N}{dt} = -v_d\frac{P_NT_N}{k_d + P_NT_N} + 2k_{in} \quad (P_2T_2)$$

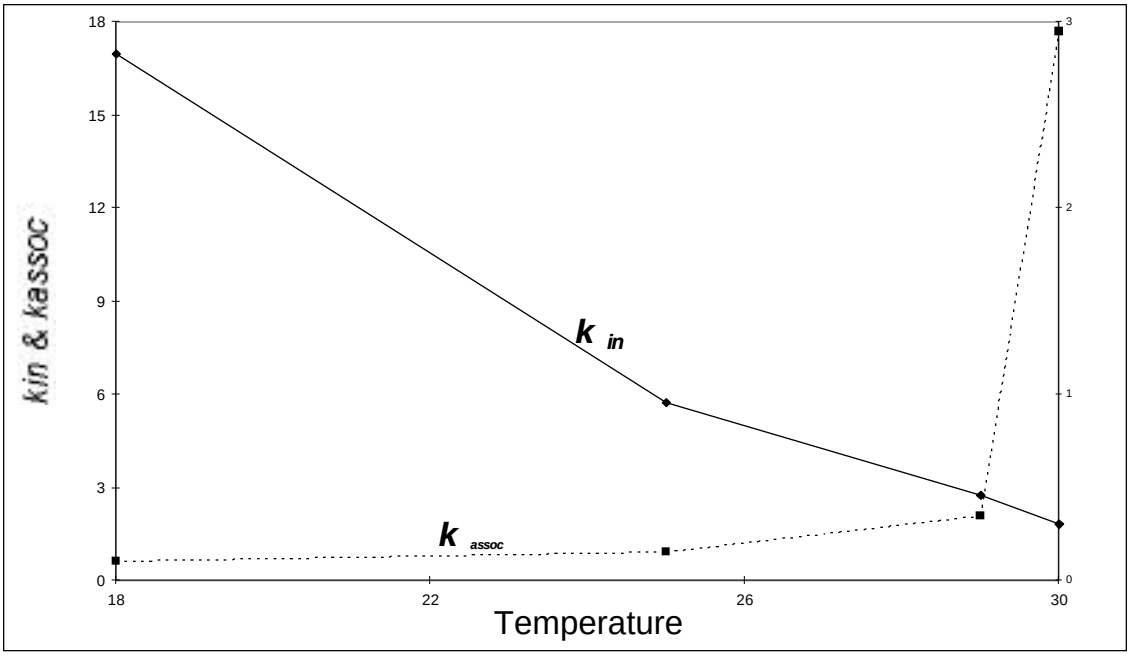

Fig. 2.5. Inverse relationship between k_{in} and temperature and direct relationship between k_{assoc} and temperature. The data points are obtained by calculating the values of k_{in} and k_{assoc} maintaining 24-h period. The dependence of k_{in} on temperature is calculated to fit observations of per^L mutant (when $k_{assoc} = 0.005$). Then the dependence of k_{assoc} on temperature is calculated so that the wild-type rhythm is 24-h at all temperatures.

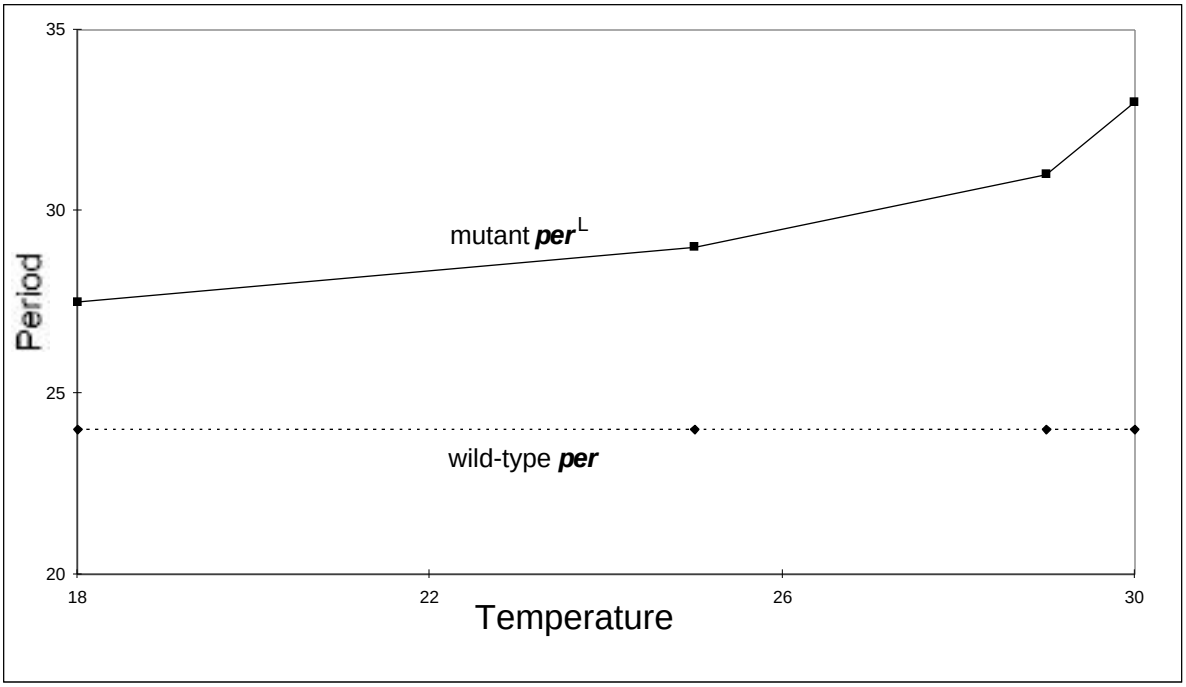

Fig. 2.6. The period of oscillations of wild-type and mutant (per^L) flies at different temperatures. The data points are taken from Huang et al. (1995), and simulated with the software AUTO. We assume that k_{in} decreases as the temperature increases causing the period to increase, and k_{assoc} increases with temperature compensating the decrease of k_{in} in wild type flies. In per^L mutant, period is sensitive to temperature because PER's ability to dimerize (k_{assoc}) is reduced.

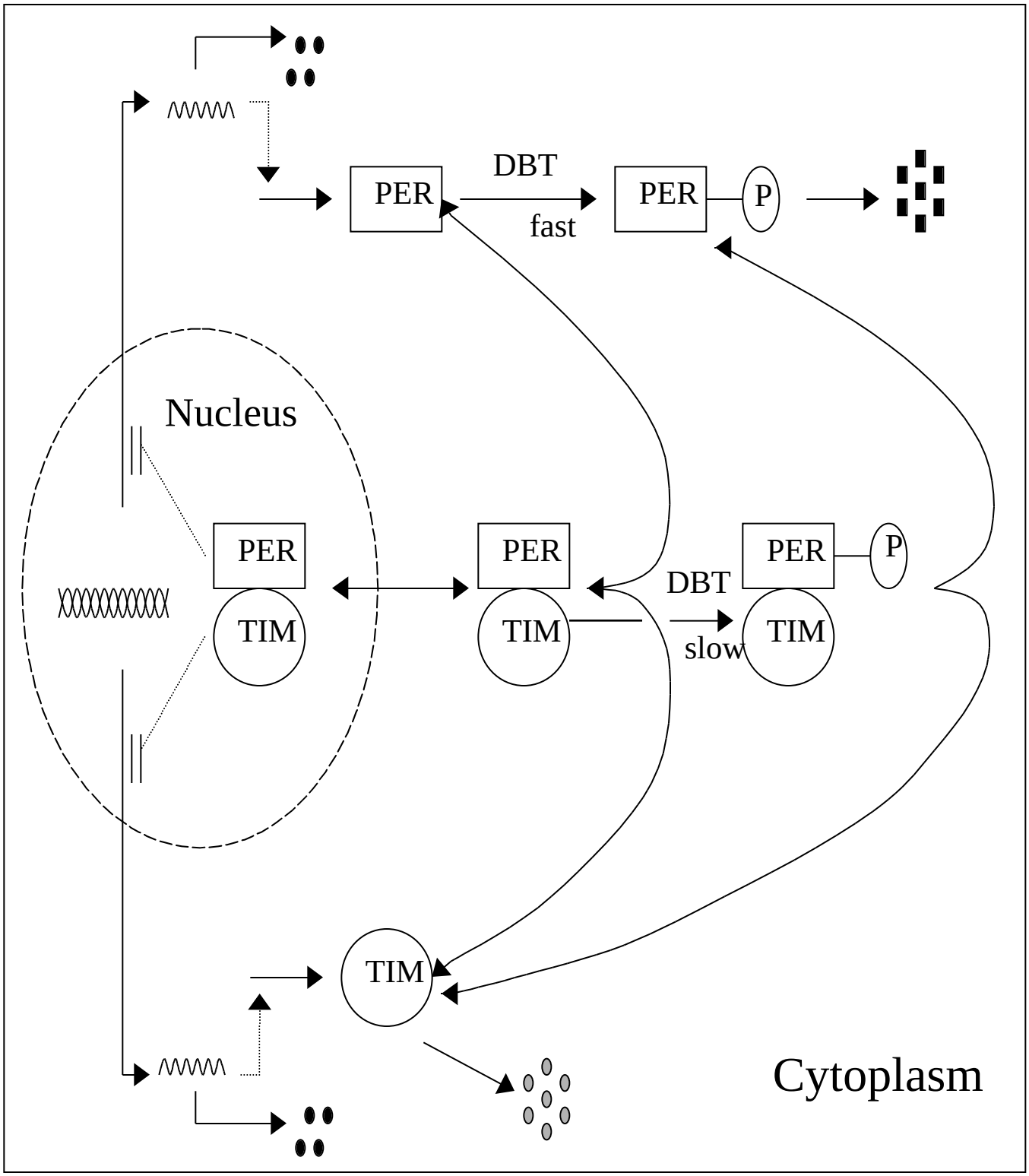

Fig. 3.1. A molecular mechanism of the circadian clock in *Drosophila* based on the interactions of PER, TIM, and DBT proteins (Price et al., 1998; Kloss et al., 1998;

Wilsbacher and Takahashi, 1998). The *per* and *tim* mRNAs are transcribed in the nucleus, and translated to PER and TIM proteins (rectangle and oval, respectively) in the cytoplasm. Both PER and TIM proteins are subject to proteolysis or they may combine to form heterodimers. We assume that monomeric PER proteins are very unstable, being rapidly degraded as soon as they are phosphorylated by DBT. Heteromeric complexes are stable and transported into the nucleus where they inhibit transcription of *per* and *tim* mRNA.

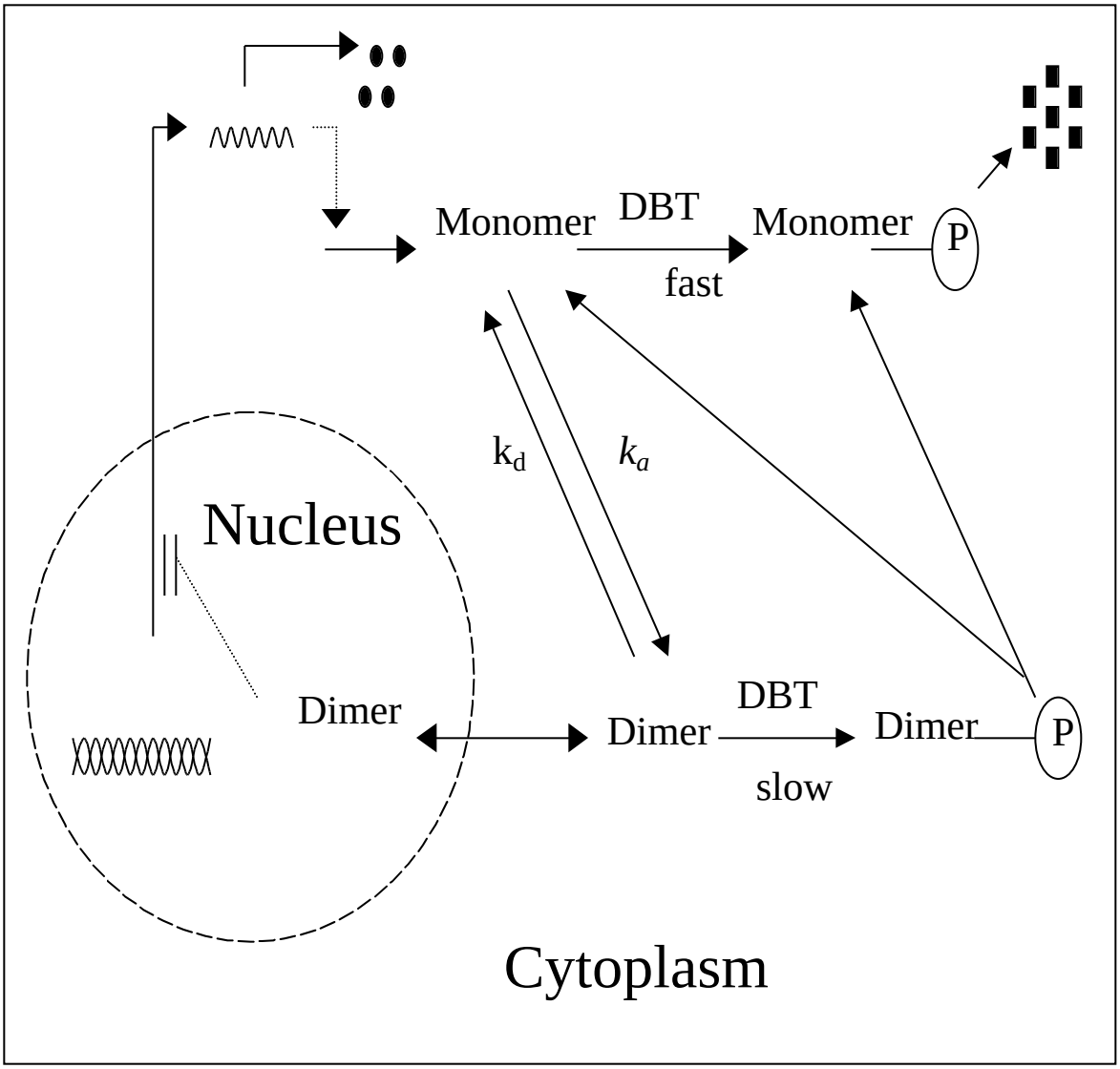

Fig. 3.2. A simplified mechanism of the circadian rhythm mechanism in *Drosophila* from figure 3.1. *per* and *tim* messages, and PER and TIM proteins are put together, and we assume that as soon as the proteins form dimers, they translocate into the nucleus and inhibit the gene transcription.

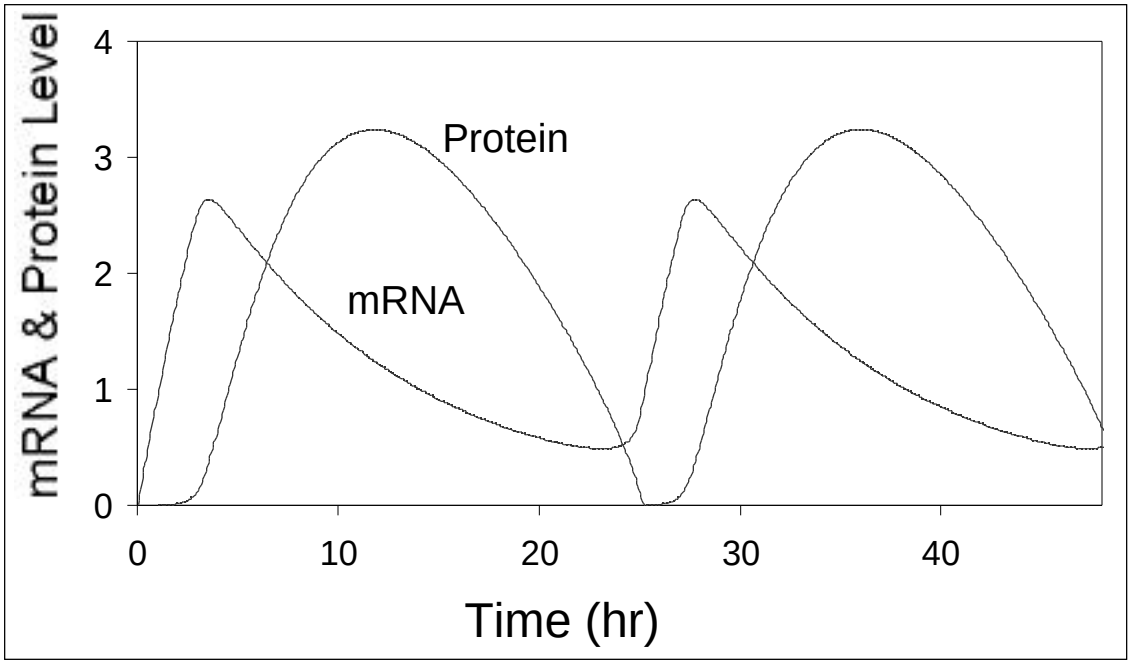

Fig. 3.3. Numerical solution of two-equation model (Eq. 5 and 6), given the parameter values in Table 3.1. mRNA and protein oscillate with 24 hour rhythm, and protein peak level is delayed about 7 hours after mRNA peak level.

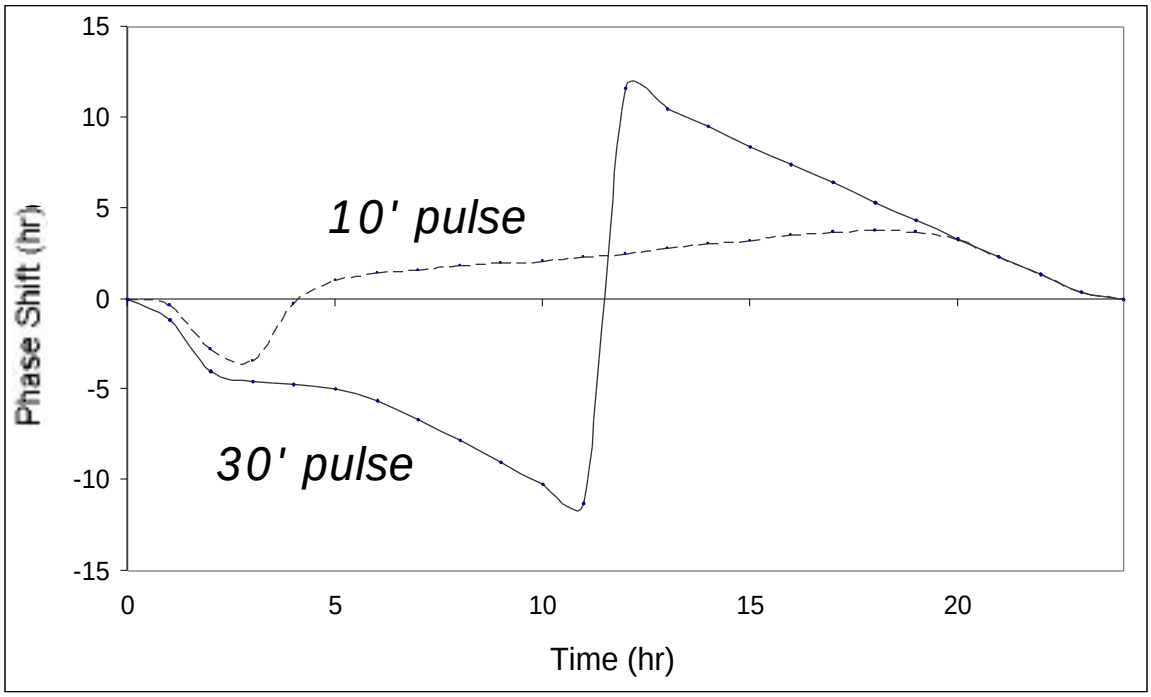

Fig. 3.4. Phase response curve. The equilibrium binding constant (K_{eq}), is reduced from 200 to 15 at a chosen phase of the endogenous rhythm for either 10 or 30 min and returned to 200. The phase difference is observed for the following 100 hours and plotted as a function of the phase at the onset of perturbation.

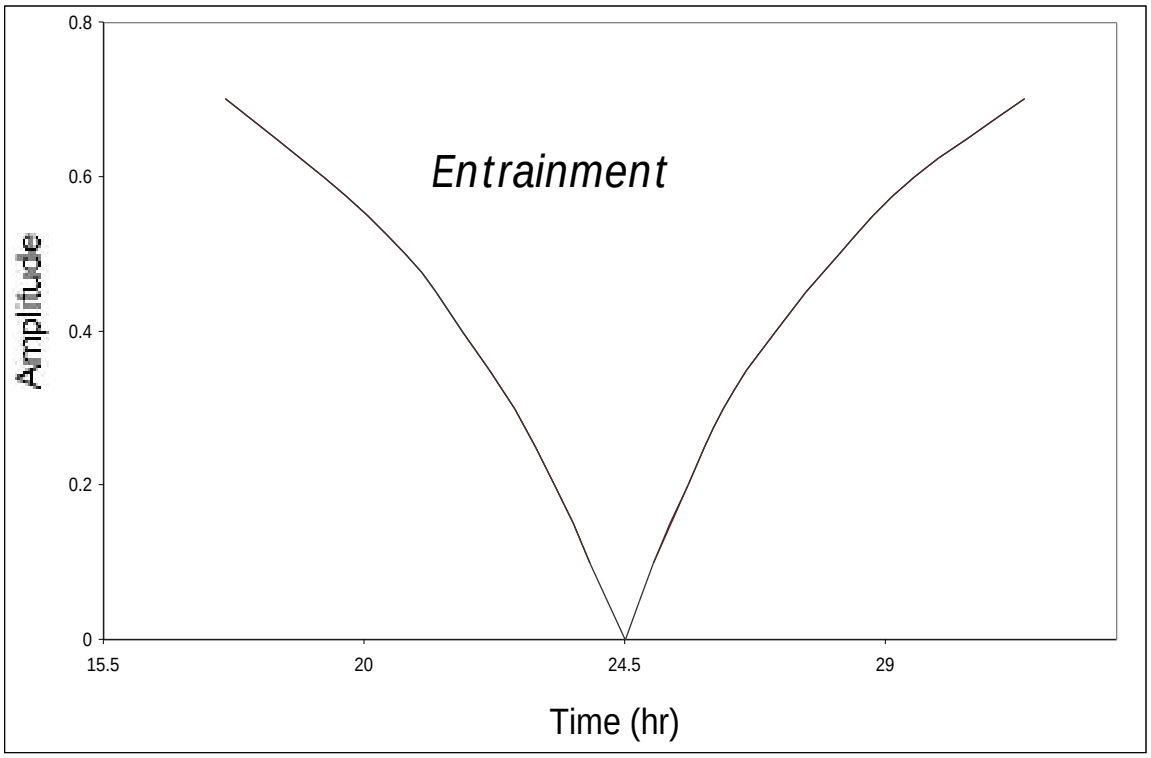

Fig. 3.5. Principal entrainment band. The equilibrium binding constant (K_{eq}) is perturbed in the equation, $q = \frac{2}{1+\sqrt{1+8K_{eq}P_t}}$, simulating the Zeitgeber period of day ($K_{eq} = 200(1-a)$) and night ($K_{eq} = 200$). The amplitude, a, represents the intensity of illumination. The minimal value of a is calculated for 1:1 entrainment of the circadian oscillator to the Zeitgeber period.

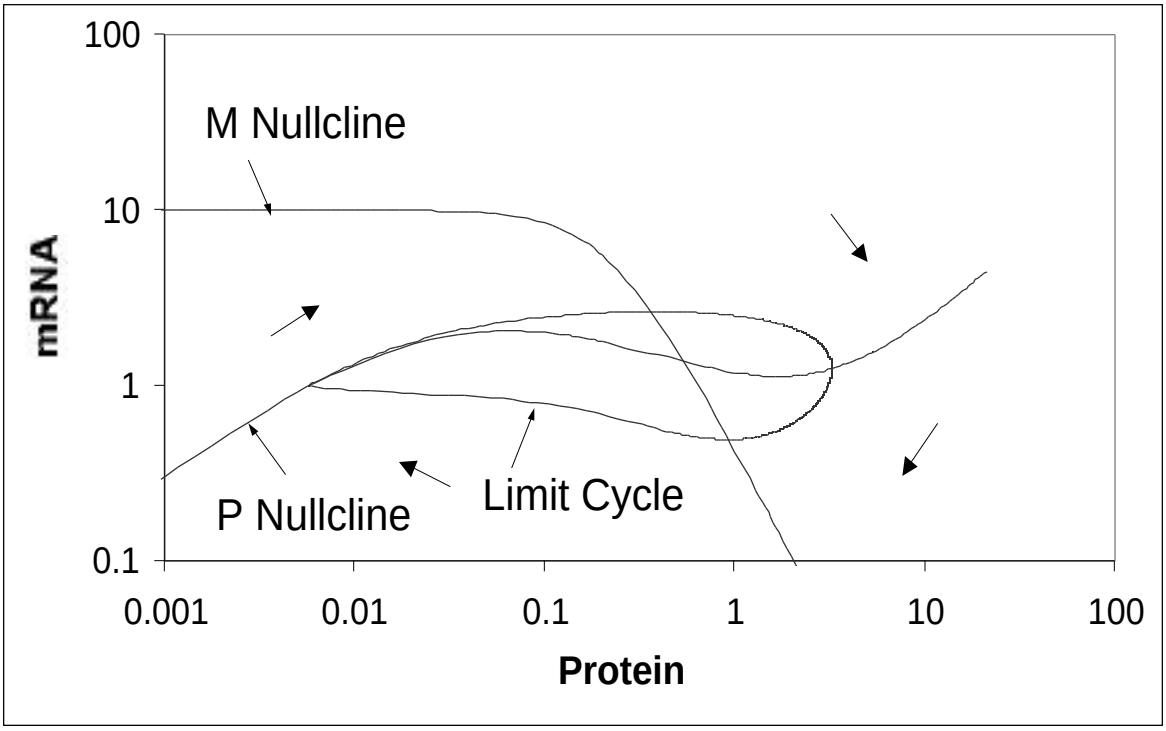

Fig. 3.6. Phase plane portraits. M and P nullclines with stable limit cycle are simulated with the parameter values in Table 3.1.

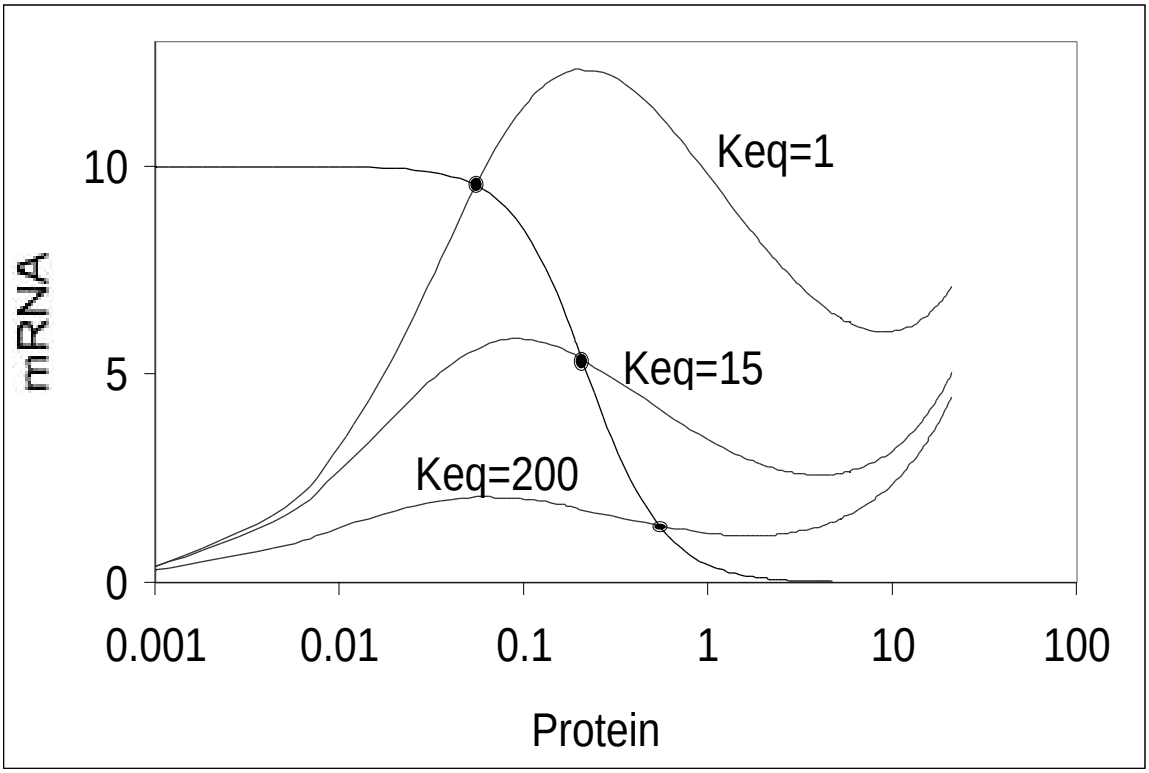

Fig. 3.7. As the equilibrium binding constant (K_{eq}) changes from 200 to 1, the P nullcline changes dramatically and creates a stable steady state when $K_{eq} = 1$.

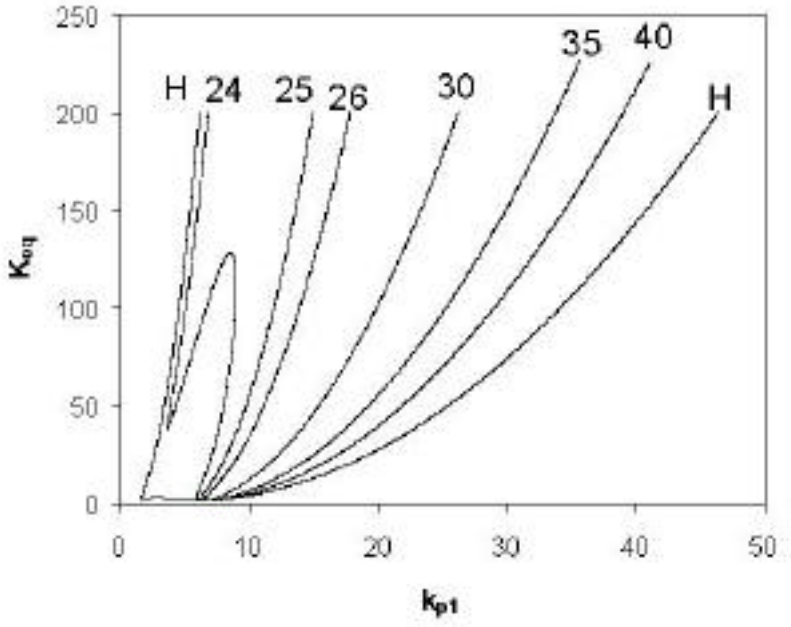

Fig. 3.8. Two-parameter bifurcation diagram for the model, calculated with the software tool AUTO (Doedel, 1986). From the stable limit cycle, we followed the region of oscillations by varying K_{eq} and k_{p1}. A U-shaped region of two-parameter space indicates where limit cycle oscillations live, bounded by a locus (H-H) of Hopf bifurcations. In this region, we indicated the existence of different periods from 24 to 40 h. The period of oscillation is quite insensitive to changes when it resides in a large region of parameter space, but then becomes very sensitive when K_{eq} is small. This calculation was done by Kalimar Maia who is doing undergraduate research in Dr. Tyson's lab.

REFERENCES

1. Allada, R., N. E. White, W. V. So, J. C. Hall, and M. Rosbash. 1998. A mutant *Drosophila* homolog of mammalian *clock* disrupts circadian rhythms and transcription of *period* and *timeless*. *Cell.* 93:791-804.
2. Darlington, T. K., K. Wager-Smith, M. F. Ceriani, D. S. Staknis, N. Gekakis, T. D. L. Steeves, C. J. Weitz, J. S. Takahashi, and S. A. Kay. 1998. Closing the Circadian Loop: CLOCK-Induced Transcription of Its Own Inhibitors *per* and *tim*. *Science.* 280:1599-1603.
3. Doedel, E. J. 1986. AUTO Software for Continuation and Bifurcation Problems in Ordinary Differential Equations. California Institute of Technology, Pasadena CA.
4. Edelstein-Keshet, L. 1988. Mathematical Models in Biology. Random House, New York.
5. Gekakis, N., L. Saez, A.-M. Delahaye-Brown, M. P. Myers, A. Sehgal, M. W. Young, and C. J. Weitz. 1995. Isolation of *timeless* by PER protein interaction: defective interaction between *timeless* protein and long-period mutant PER^{L}. *Science.* 270:811-815.
6. Goldbeter, A. 1995. A model for circadian oscillations in the *Drosophila* period protein (PER). *Proc. Royal Soc. Lond. B.* 261:319-324.
7. Hardin, P. E., J. C. Hall, and M. Rosbash. 1992. Circadian oscillations in *period* gene mRNA levels are transcriptionally regulated. *Proc. Natl. Acad. Sci. USA.* 89:11711-11715.
8. Hardin, P. E., J. C. Hall, and M. Rosbash. 1990. Feedback of the *Drosophila period* gene product on circadian cycling of its messenger RNA levels. *Nature.* 343:536-540.
9. Huang, Z. J., K. D. Curtin, and M. Rosbash. 1995. PER protein interactions and temperature compensation of a circadian clock in *Drosophila*. *Science.* 267:1169-1172.

10. Hunter-Ensor, M., A. Ousley, and A. Sehgal. 1996. Regulation of the Drosophila protein timeless suggests a mechanism for resetting the circadian clock by light. *Cell.* 84:677-685.

11. Kloss, B., J. L. Price, L. Saez, J. Blau, A. Rothenfluh, C. S. Wesley, and M. W. Young. 1998. The *Drosophila* clock gene *double-time* encodes a protein closely related to human casein kinase 1ε. *Cell.* 94:97-107.

12. Konopka, R. J., and S. Benzer. 1971. Clock mutants of *Drosophila melanogaster*. *Proc. Natl. Acad. Sci. USA.* 68:2112-2116.

13. Lee, C., V. Parikh, T. Itsukaichi, K. Bae, and I. Edery. 1996. Resetting the *Drosophila* clock by photic regulation of PER and a PER-TIM complex. *Science.* 271:1740-1744.

14. Myers, M. P., K. Wager-Smith, A. Rothenfluh-Hilfiker, and M. W. Young. 1996. Light-induced degradation of TIMELESS and entrainment of the *Drosophila* circadian clock. *Science.* 271:1736-1740.

15. Myers, M. P., K. Wager-Smith, C. S. Wesley, M. W. Young, and A. Sehgal. 1995. Positional cloning and sequence analysis of the *Drosophila* clock gene, *timeless*. *Science.* 270:805-810.

16. Pittendrigh, C. S. 1967. Circadian systems, I. The driving oscillation and its assay in *Drosophila pseudoobscura*. *Proc. Natl. Acad. Sci. USA.* 58:1762-1767.

17. Price, J. L., J. Blau, A. Rothenfluh, M. Abodeely, B. Kloss, and M. W. Young. 1998. *double-time* is a novel *Drosophila* clock gene that regulates PERIOD protein accumulation. *Cell.* 94:83-95.

18. Ruoff, P., L. Rensing, R. Kommedal, and S. Mohsenzadeh. 1997. Modeling temperature compensation in chemical and biological oscillators. *Chronobiol. Internat.* 14:499-510.

19. Ruoff, P., and L. Rensing. 1996. The temperature-compensated Goodwin model simulates many circadian clock properties. *J. Theor. Biol.* 179:275-285.

20. Ruoff, P. 1992. Introducing temperature-compensation in any reaction kinetic oscillator. *J. Interdiscipl. Cycle Res.* 23:92-99.

21. Rutila, A. E., V. Suri, M. Le, W. V. So, M. Rosbash, and J. C. Hall. 1998. CYCLE is a second bHLH-PAS clock protein essential for circadian rhythmicity and transcription of *Drosophila period* and *timeless*. *Cell.* 93:805-814.

22. Sehgal, A., A. Rothenfluh-Hilfiker, M. Hunter-Ensor, Y. Chen, M. P. Myers, and M. W. Young. 1995. Rhythmic expression of *timeless*: a basis for promoting circadian cycles in *period* gene autoregulation. *Science.* 270:808-810.

23. Sehgal, A., J. L. Price, B. Man, and M. W. Young. 1994. Loss of circadian behavioral rhythms and *per* RNA oscillations in the *Drosophila* mutant *timeless*. *Science.* 263:1603-1606.

24. Smith, R. F., and R. J. Konopka. 1982. Effects of Dosage Alterations at the *per* Locus on the Period of the Circadian Clock of *Drosophila*. *Mol. Gen. Genet.* 185:30-36.

25. Vosshall, L. B., J. L. Price, A. Sehgal, L. Saez, and M. W. Young. 1994. Block in nuclear localization of *period* protein by a second clock mutation, *timeless*. *Science.* 263:1606-1609.

26. Wilsbacher, L. D., and J. S. Takahashi. 1998. Circadian rhythms: molecular basis of the clock. *Curr. Opin. Gen. Devel.* 8:595-602.

27. Zeng, H., Z. Qian, M. Myers, and M. Rosbash. 1996. A light-entrainment mechanism for the *Drosophila* circadian clock. *Nature.* 380:129-135.

28. Zeng, H., P. E. Hardin, and M. Rosbash. 1994. Constitutive overexpression of the *Drosophila* period protein inhibits *period* mRNA cycling. *EMBO J.* 13:3590-3598.